ERDC/CRREL TR-20-4

Cold Regions Research
and Engineering Laboratory

US Army Corps
of Engineers®
Engineer Research and
Development Center

ERDC
ENGINEER RESEARCH & DEVELOPMENT CENTER

Engineering for Polar Operations, Logistics, and Research (EPOLAR)

A Generalized Approach for Modeling Creep of Snow Foundations

Devin T. O'Connor and Robert B. Haehnel

May 2020

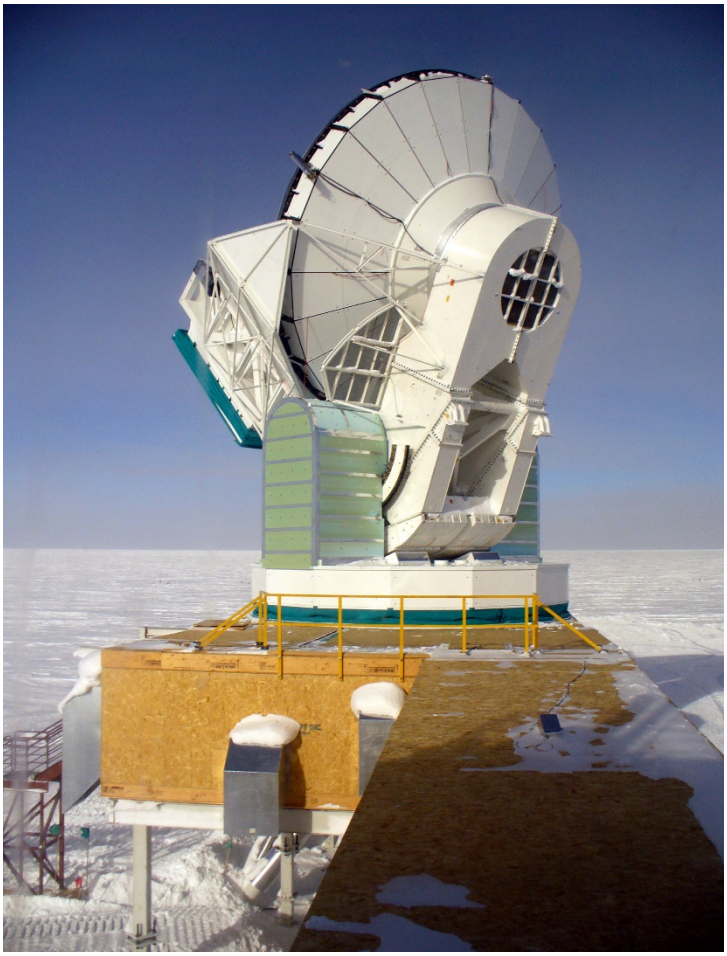

The U.S. Army Engineer Research and Development Center (ERDC) solves the nation's toughest engineering and environmental challenges. ERDC develops innovative solutions in civil and military engineering, geospatial sciences, water resources, and environmental sciences for the Army, the Department of Defense, civilian agencies, and our nation's public good. Find out more at www.erdc.usace.army.mil.

To search for other technical reports published by ERDC, visit the ERDC online library at https://erdclibrary.on.worldcat.org/discovery.

Cover image: South Pole Telescope. Photograph courtesy of Wikimedia Commons, https://commons.wikimedia.org/wiki/File:South_pole_telescope_nov2009.jpg#globalusage.

ERDC/CRREL TR-20-4
May 2020

A Generalized Approach for Modeling Creep of Snow Foundations

Devin T. O'Connor and Robert B. Haehnel

U.S. Army Engineer Research and Development Center (ERDC)
Cold Regions Research and Engineering Laboratory (CRREL)
72 Lyme Road
Hanover, NH 03755-1290

Final Report

Prepared for National Science Foundation, Office of Polar Programs
Antarctic Infrastructure and Logistics
2415 Eisenhower Avenue
Alexandria, VA 22314

Under Engineering for Polar Operations, Logistics, and Research (EPOLAR)
EP-ANT-18-85, "A Generalized Approach for Modeling Creep of Snow Foundations"

Abstract

When an external load is applied, snow will continue to deform in time, or creep, until the load is removed. When using snow as a foundation material, one must consider the time-dependent nature of snow mechanics to understand its long-term structural performance. In this work, we develop a general approach for predicting the creep behavior of snow. This new approach spans the primary (nonlinear) to secondary (linear) creep regimes. Our method is based on a uniaxial rheological Burgers model and is extended to three dimensions. We parameterize the model with density- and temperature-dependent constants that we calculate from experimental snow creep data. A finite element implementation of the multiaxial snow creep model is derived, and its inclusion in an ABAQUS user material model is discussed. We verified the user material model against our analytical snow creep model and validated our model against additional experimental data sets. The results show that the model captures the creep behavior of snow over various time scales, temperatures, densities, and external loads. By furthering our ability to more accurately predict snow foundation movement, we can help prevent unexpected failures and extend the useful lifespan of structures that are constructed on snow.

Contents

Figures and Tables

Figures

Tables

Preface

This study was conducted for the National Science Foundation, Office of Polar Programs, Antarctic Infrastructure and Logistics (NSF-OPP-AIL), under Engineering for Polar Operations, Logistics, and Research (EPOLAR) EP-ANT-18-85, "A Generalized Approach for Modeling Creep of Snow Foundations." The technical monitor was Ms. Margaret Knuth, Operations Manager, NSF-OPP-AIL, U.S. Antarctic Program.

The work was performed by the Terrestrial and Cryospheric Sciences Branch of the Research and Engineering Division, U.S. Army Engineer Research and Development Center, Cold Regions Research and Engineering Laboratory (ERDC-CRREL). At the time of publication, Dr. John Weatherly was Branch Chief; Mr. J. D. Horne was Division Chief; and Dr. Martin Jeffries was the Technical Director for Cold Regions Science and Engineering. The Deputy Director of ERDC-CRREL was Mr. David B. Ringelberg, and the Director was Dr. Joseph L. Corriveau.

COL Teresa A. Schlosser was the Commander of ERDC, and Dr. David W. Pittman was the Director.

1 Introduction

1.1 Background

When building structures on snow foundations, one has to consider the time-dependent deformation of the snow under loading. If a long-term load from a permanent structure or installation is applied, the snow will creep, or deform, at a time-dependent rate. The rate of deformation can depend on, for example, the current microstructure, density, and temperature of the snowpack (Theile et al. 2011; Salm 1982; Mellor and Smith 1966). Generally, the creep of snow to a constant external loading or stress is described in three stages. First, there is a *primary regime* that contains the instantaneous elastic response of the snow to a loading and a subsequent nonlinear time-dependent decelerating strain rate. In the next regime, the *secondary regime*, the strain rate of the snow becomes constant in time. Lastly, in the *tertiary regime,* the strain rate of the snow increases until failure. See Haehnel (2017) for an example of a typical uniaxial creep curve with constant loading and Salm (1982), Mellor (1975, 1964), and Shapiro et al. (1997) for a review of the mechanics of snow, including creep.

Most often, structures placed on snow foundations will encounter the first two regimes of creep (primary and secondary). The deformation of the foundation during primary and secondary creep is most relevant during shorter-term loading, while the strain in the secondary regime typically dominates most of the deformation for long-term loading. In our work, the general model for creep deformation of snow foundations combines the features of primary and secondary creep to predict snow foundation deformation under short- and long-term loading.

Two common approaches model the mechanics of snow at the macroscopic scale. The first, rheological models, usually consist of spring-dashpot systems connected in series or parallel to represent the linear viscoelastic behavior of snow. Examples of rheological models include the two-parameter Maxwell (Bartelt and Christen 2007; Teufelsbauer 2011) and Kelvin-Voigt models (Kozin et al. 2013); the three-element model (Kelvin-Voigt model with an elastic spring in series); and a four-parameter Burgers material model (Yoshida 1955) that consists of a linear spring, a viscous damper, and a spring and damper in parallel. Each unit of the rheological models (e.g., springs, dashpots, and combinations thereof) is assembled in

a specific way to capture the mechanics of snow. Mellor (1975) further reviews the different rheological approaches. The second modeling approach, microstructure-based techniques, explicitly resolve the porous microstructure of the snow and develop the constitutive response of the snow based on its representative microstructure (Chandel et al. 2014; Köhle and Schneebeli 2014; Srivastava et al. 2016).

Other methods to model snow include the discrete element method (Ghaboussi and Barbosa 1990), which represents snow grains as discrete rigid particles and defines their interactions by local particle-to-particle contact laws (Vedachalam et al. 2011; Johnson and Hopkins 2005; Hagenmuller et al. 2015). Our work leverages the rheological modeling approach to represent the viscoelastic response of snow in the primary and secondary regimes of creep.

Mellor and Smith (1966) lead initial attempts to model the creep of snow and ice, developing models for the secondary regime of creep (constant strain rate) and assuming the behavior to follow an Arrhenius relation with activation energies for secondary creep depending on apparent density. Navarre et al. (2007) presented a three-dimensional model of snow deformation, based on a nonlinear viscous constitutive model, with the parameters of the model depending on the density and temperature of the snow. Chandel et al. (2007) developed a rheological model for snow creep by using a four-parameter Burgers model. The model parameters were dependent on the density and were determined from creep experiments on snow, but the model did not include the temperature dependence of these parameters. Teufelsbauer (2011) developed a two-dimensional model of the long-term creep of alpine snow packs and treats the snow as a compressible viscous fluid.

Haehnel (2017) formulated a more general model for creep of dense snow (440–890 kg/m^3) under a static applied load by extending the formulation by Mellor and Smith (1966). The Haehnel (2017) model was developed to apply only to the primary and secondary regimes of creep during foundation settlement on snow. Potentially restricting its application, it presented two independent models to simulate the first two regimes of creep instead of a unified model that could span both regimes.

To understand snow foundation settlement, it is advantageous to develop a combined model that spans the response from primary to secondary

creep. Frequently, foundation applications span the transition from primary creep deformation to secondary creep over the operational life span, and a model that captures the transition will better characterize overall foundation performance. Because tertiary creep indicates the beginning of foundation failure, models need not cover this creep regime.

1.2 Objective

In this work, we develop a rheological model for snow creep that is based on the four-parameter Burgers model and extend the model by accounting for the temperature and density dependence of snow in our parameterization. Therefore, our approach considers long-term foundation performance for a range of snow temperatures and densities characteristic of polar regions.

1.3 Approach

We begin this report by presenting the development of our multiaxial snow creep model and its implementation into a commercial finite element code. A one-dimensional version of our model is derived in section 2.3, and we estimate the values for the parameters used in our model by minimizing the difference between our simulation results and experimental uniaxial snow creep data (Meussen et al. 1999; Chandel et al. 2007; Mellor and Smith 1966). In section 3, we verify our finite element implementation against analytical snow creep values; and section 4 presents our modeling results in comparison with experimental data. Lastly, section 5 provides some additional discussion and conclusions.

2 Computational Methods

2.1 Snow constitutive model

The model developed in this work is based on the four-parameter Burgers rheological model that consists of an elastic spring with modulus E_0, a damper with viscosity μ_0, and a Kelvin unit with a spring and damper in parallel. See Figure 1 for an example of the one-dimensional Burgers model.

Figure 1. One-dimensional Burgers model.

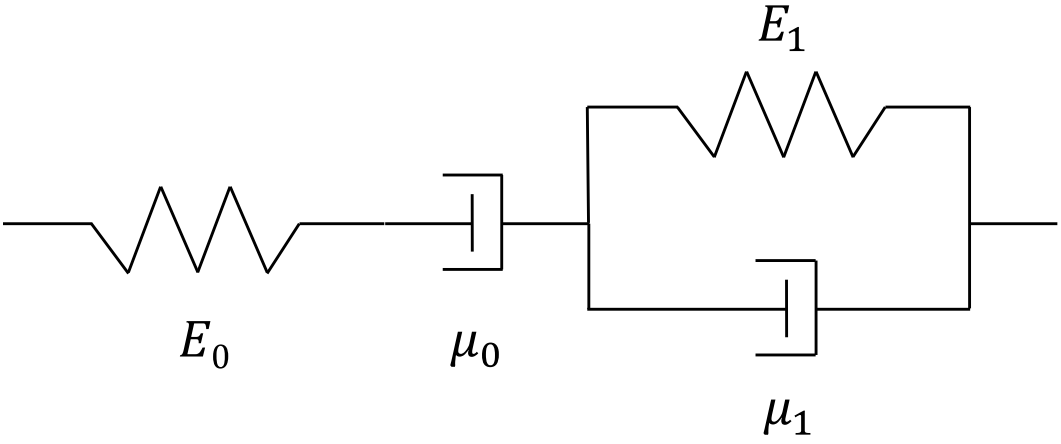

The rheological Burgers model captures the primary and secondary creep behavior of snow. Note that our work does not consider material failure, so this report models only the primary and secondary regimes of creep. In the primary regime, there is an initial elastic strain response, modeled with the spring constant E_0, and an unrecoverable time-dependent strain response modeled with the combination of the single damper and the Kelvin unit. After a time dependent on the values of the model parameters, secondary creep dominates, and the strain response is determined mostly by the behavior of the damper with viscosity μ_0. Most approaches to modeling the creep of snow calibrate these parameters against experimental data. See Chandel et al. (2007) for an example.

In our approach to modeling snow creep, we extend the Burgers model to three dimensions and assume the model parameters are dependent on the temperature and density of the snowpack at any given time. We base our multiaxial extension of the Burgers model on models of ice by Xu et al. (2019), Duddu and Waisman (2012, 2013), and Londono et al. (2016). The

model can be broken down into three strain contributions: a time-independent recoverable elastic strain, a time-dependent recoverable delayed strain, and a time-dependent, unrecoverable viscous strain. Assuming small strain and summing all strain contributions, the total strain is

$$\varepsilon_{ij} = \varepsilon_{ij}^{e} + \varepsilon_{ij}^{d} + \varepsilon_{ij}^{v}, \tag{1}$$

where the superscript e stands for elastic, d stands for delayed, and v stands for viscous. The strain ε is a second-order tensor, and the subscripts i and j refer to components of the tensor. Throughout the manuscript, we will use tensor notation, sometimes referred to as Einstein notation. Note that when there are repeated indices (e.g., σ_{kk}), the quantity is summed. For example, $\sigma_{kk} = \sigma_{11} + \sigma_{22} + \sigma_{33}$ if k has 3 components. The Cauchy stress of the snow is a function of the elastic strain and is defined as

$$\sigma_{ij} = C_{ijkl}\varepsilon_{ij}^{e}, \tag{2}$$

where C_{ijkl} is the fourth-order elasticity tensor given by

$$C_{ijkl} = \lambda(\rho, T)\delta_{ij}\delta_{kl} + \mu(\rho, T)\left(\delta_{ik}\delta_{jl} + \delta_{il}\delta_{jk}\right). \tag{3}$$

The elastic material parameters λ and μ are referred to as Lamé parameters, and δ_{ij} is the identity tensor. The Lamé parameters are functions of the usual modulus of elasticity, E, and Poisson's ratio, ν, that are used to define elastic materials. Note that in our modeling approach, the Lamé parameters are functions of the density, ρ, and temperature, T. That is because we define our elastic modulus to be a function of those two variables. Section 2.3.1 will discuss the functional form of the elastic modulus.

The delayed elastic strain is usually defined in rate form and is given by

$$\dot{\varepsilon}^{d}{}_{ij} = A(\rho, T)\left(\frac{3}{2}K(\rho)S_{ij} - \varepsilon_{ij}^{d}\right), \tag{4}$$

where A is a density- and temperature-dependent constant, K is a density-dependent constant defined from experimental data, and

$$S_{ij} = \sigma_{ij} - \frac{1}{3}\sigma_{kk}\delta_{ij} \tag{5}$$

is the deviatoric stress tensor. Inspired by the work of Haehnel (2017) and Mellor (1964), we extend the work of Ohno et al. (1985) and Karr and Choi

(1989) and modify the parameter A to have an Arrhenius relationship with density and temperature:

$$A(\rho, T) = A_0(\rho) \exp\left(-\frac{Q(\rho)}{RT}\right), \tag{6}$$

where A_0 is a density-dependent constant found from experimental data, R is the gas constant, and T is the temperature of the snow foundation. The density-dependent activation energy, Q, is also found using experimental data as discussed in section 2.3.2.

The time-dependent, unrecoverable viscous strain is also usually defined in rate form as

$$\dot{\varepsilon}_{ij}^{v} = \frac{3}{2} B(\rho, T) S_{ij} \left(\frac{3}{2} S_{kl} S_{kl}\right)^{\frac{n-1}{2}}, \tag{7}$$

where B is a density and temperature-dependent constant and n is a viscous-strain exponent we set to be equal to one ($n = 1$) as did Haehnel (2017). Parameter B takes on a form similar to that of equation (6):

$$B(\rho, T) = B_0(\rho) \exp\left(-\frac{Q(\rho)}{RT}\right), \tag{8}$$

where B_0 is a density- and temperature-dependent constant that is defined using experimental data as explained in section 2.3.3. Note that for the density-dependent constants, defined above, we use a temporally constant density since our method currently does not allow the density to change in time.

Assuming a rate form, the Cauchy stress in the snow is defined as

$$\dot{\sigma}_{ij} = C_{ijkl}\left(\dot{\varepsilon}_{kl} - \dot{\varepsilon}_{kl}^{d} - \dot{\varepsilon}_{kl}^{v}\right), \tag{9}$$

where the definitions for the strain rates have been defined previously. We will use this definition for the stress rate in the snow to create our finite element implementation in the next section.

2.2 Finite element implementation

We implemented our snow creep model in the commercial finite element software ABAQUS by creating a user material model subroutine (see Appendix A for the Fortran code). Given the current state of the simulation at a particular time (e.g., strain, temperature, etc.), the subroutine requires the user to define an increment in stress and a material tangent modulus over the given time increment. Using the rate form of the Cauchy stress shown in equation (9) and assuming the response of the material is linear over a given time increment, we can multiply the stress rate by the time increment Δt to define an increment in stress,

$$\Delta\sigma_{ij} = C_{ijkl}\left(\Delta\varepsilon_{kl} - \Delta\varepsilon_{kl}^{d} - \Delta\varepsilon_{kl}^{v}\right), \tag{10}$$

with the definitions for the delayed and viscous-strain increments given by

$$\Delta\varepsilon_{kl}^{d} = A(\rho,T)\Delta t\left(\frac{3}{2}K(\rho)S_{ij} - \varepsilon_{ij}^{d}\right), \tag{11}$$

$$\Delta\varepsilon_{kl}^{v} = \frac{3}{2}B(\rho,T)\Delta t S_{ij}\left(\frac{3}{2}S_{kl}S_{kl}\right)^{\frac{n-1}{2}}. \tag{12}$$

The tangent modulus is easily found by taking the derivative of the increment in stress by an increment in strain. Therefore, the tangent modulus was found to be

$$\Pi_{ijkl} = \frac{\partial\Delta\sigma_{ij}}{\partial\Delta\varepsilon_{kl}} = C_{ijkl}. \tag{13}$$

Appendix A shows the full snow creep model, including the implementations of the stress increment and tangent modulus.

2.3 Model parameter estimation

To estimate the parameters of the snow creep model laid out in the previous sections, we compare our model to uniaxial constant stress creep tests. We use three different data sets from Chandel et al. (2007), Meussen et al. (1999), and Mellor and Smith (1966). To compare with the experimental data, we simplify our uniaxial model to one dimension and solve for the total strain rate:

$$\dot{\varepsilon}(\mathrm{t}) = \frac{\dot{\sigma}(t)}{E(\rho)} + A(\rho,T)(K(\rho)\sigma(t) - \varepsilon^{d}) + B(\rho,T)\sigma(t)^{n}. \tag{14}$$

Assuming a constant stress rate in time, $\sigma(t) = \sigma_0$, we can analytically integrate the strain rate to define the time-dependent total strain:

$$\varepsilon(t) = \frac{\sigma_0}{E(\rho)} + K(\rho)(\sigma_0(1 - \exp(-A(\rho,T)t)) + B(\rho,T)\sigma_0^n t. \quad (15)$$

This analytical equation is used to compare the creep strain with the experimental data sets and to calculate model parameters. Section 2.3.3 details calculating the model parameters. Additionally, we use experimental data sets to define the density-dependent elastic modulus (section 2.3.1) and activation energy (section 2.3.2).

2.3.1 Elastic properties of snow

Because of the microscale structure of snow, the apparent or measured elastic modulus can change with density. In our model, we assume the elastic modulus (i.e., Young's modulus) of snow has a power-law relationship with density:

$$E(\rho) = E_1 \rho^{E_2}, \quad (16)$$

where ρ is density and E_1 and E_2 are constants that are determined from experimental data.

Mellor (1975) collected from numerous experiments values for the Young's modulus of dense coherent dry snow. To calculate our elastic material constants, we used a subset of the Mellor (1975) experimental data that was collected using pulse propagation or flexural vibration at high frequencies at temperatures of −10°C to −25°C. Using a least-squares fitting routine to match the experimental data, we calculated $E_1 = 1.99884211 \times 10^{-6}$ and $E_2 = 5.307$ with an R^2 value of 0.99. Figure 2 shows the experimental Young's modulus data and the model results.

Figure 2. Density-dependent elastic modulus model plotted against experimental elastic modulus data.

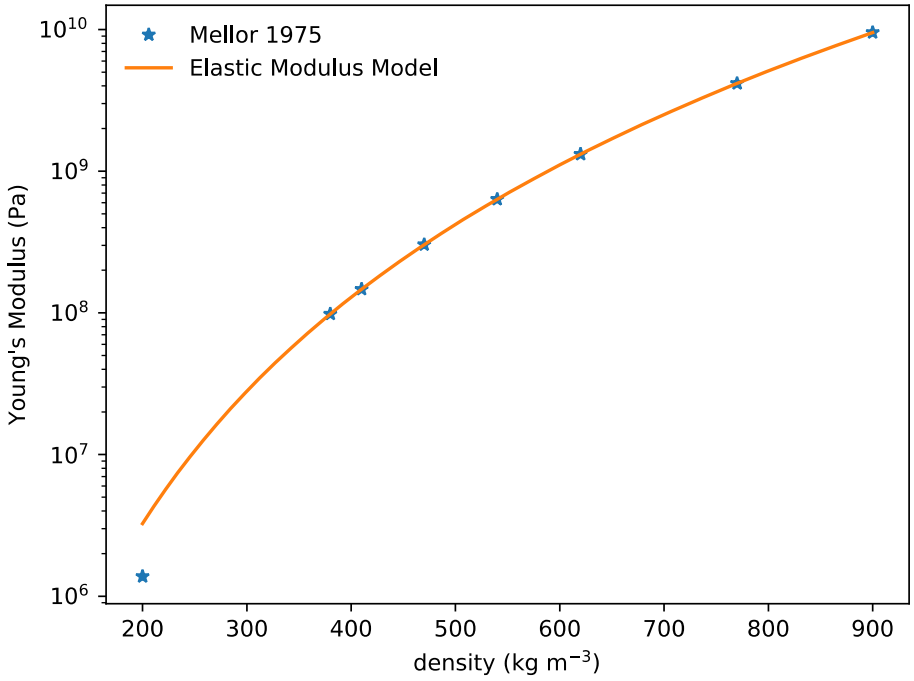

2.3.2 Activation energy

We follow the work of Mellor and Smith (1966) and assume that the creep of snow is a thermally activated process that follows an Arrhenius relationship. Mellor and Smith performed snow creep tests with snow of varying densities, at different temperatures, and with different applied loads. Assuming a functional form of the creep strain rate, they calculated an activation energy as a function of density. See Mellor and Smith (1966) for the table of density-dependent activation-energy values. Based on their data, we assumed the activation energy followed a power-law relationship with density:

$$Q(\rho) = Q_1 \rho^{Q_2}, \tag{17}$$

where Q_1 and Q_2 are constants that we calculated based on the data. To find the constants, we performed a least-squares fitting with the data and found values of $Q_1 = 1145.23$ and $Q_2 = -0.69$ with an R^2 value of 0.93.

Figure 3 shows the snow creep activation-energy model compared with the activation-energy data. Note that the activation-energy model comes into the snow creep model through equations (6) and (8).

Figure 3. Snow creep activation energy as a function of density.

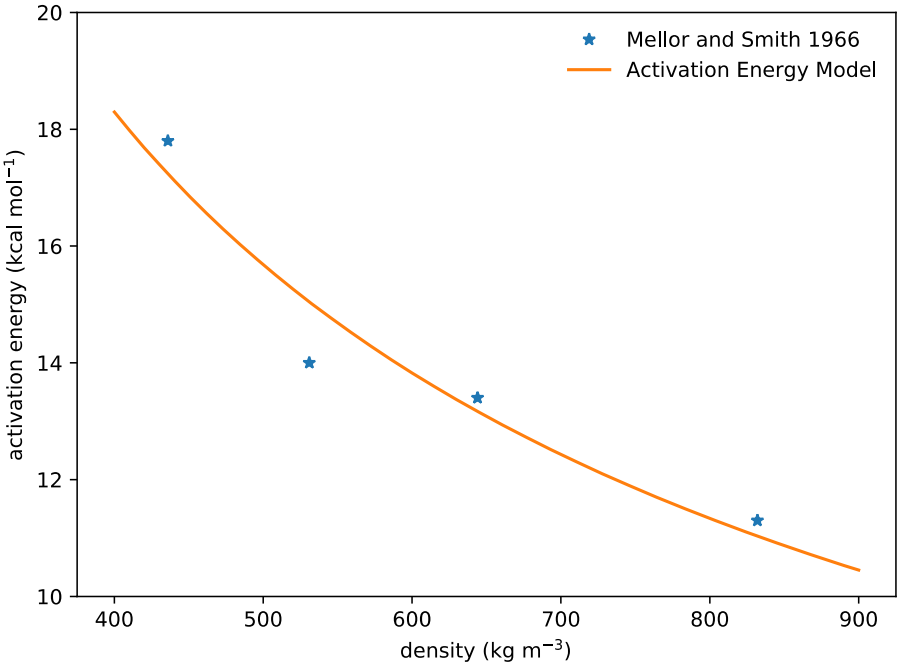

2.3.3 Empirical constants

To complete the parameterization of the model, we calculated the values for $A_0(\rho)$, $B_0(\rho)$, and $K(\rho)$ seen in equations (6), (8), and (4) that best fit experimental data. We used the uniaxial unconfined snow creep compression tests from Meussen et al. (1999), Chandel et al. (2007), and Mellor and Smith (1966) as our experimental data sets to estimate model parameters. The works by Meussen et al. (1999) and Chandel et al. (2007) both reported creep strain results that included nonlinear effects for different combinations of compressive axial load, snow density, and temperature while Mellor and Smith (1996) reported constant compressive strain rate results characteristic of the secondary creep regime.

We assumed a power-law functional form for the constants $A_0(\rho)$, $B_0(\rho)$, and $K(\rho)$ seen in the following equations:

$$A_0(\rho) = A_{01}\rho^{A_{02}}, \tag{18}$$

$$B_0(\rho) = B_{01}\rho^{B_{02}}, \tag{19}$$

$$K(\rho) = K_1\rho^{K_2}, \tag{20}$$

where A_{01}, A_{02}, B_{01}, B_{02}, K_1, and K_2 are constants found from fitting to experimental data. We first used the strain and strain-rate predictions from our creep model and a least-squares fitting routine to find the values for the parameters in the previous three equations that best fit the experimental data.

Figures 4, 5, and 6 show model results using parameters estimated from a least-squares fitting to the experimental data. As seen in the figures, the creep model captures the response of the snow quite well from the initial nonlinear strain response through a constant secondary creep-like strain rate. Although, the model does not capture the strain rate as well for the Mellor and Smith (1966) data set for a density of approximately 550 kg m^{-3}. This strain-rate response is characteristic across all temperatures at that density tested but does not follow the overall trend of the strain rate, where it is expected to be more or less linear. From the least-squares fitting to the experimental data, we collected all of the estimated values for $A_0(\rho)$, $B_0(\rho)$, and $K(\rho)$ as a function of density.

Figure 4. Creep-model predictions (*solid line*) of strain against the experimental data set from Meussen et al. (1999) (*asterisks*) for a variety of snow densities and external loads. The snow temperature was −20 °C for all samples.

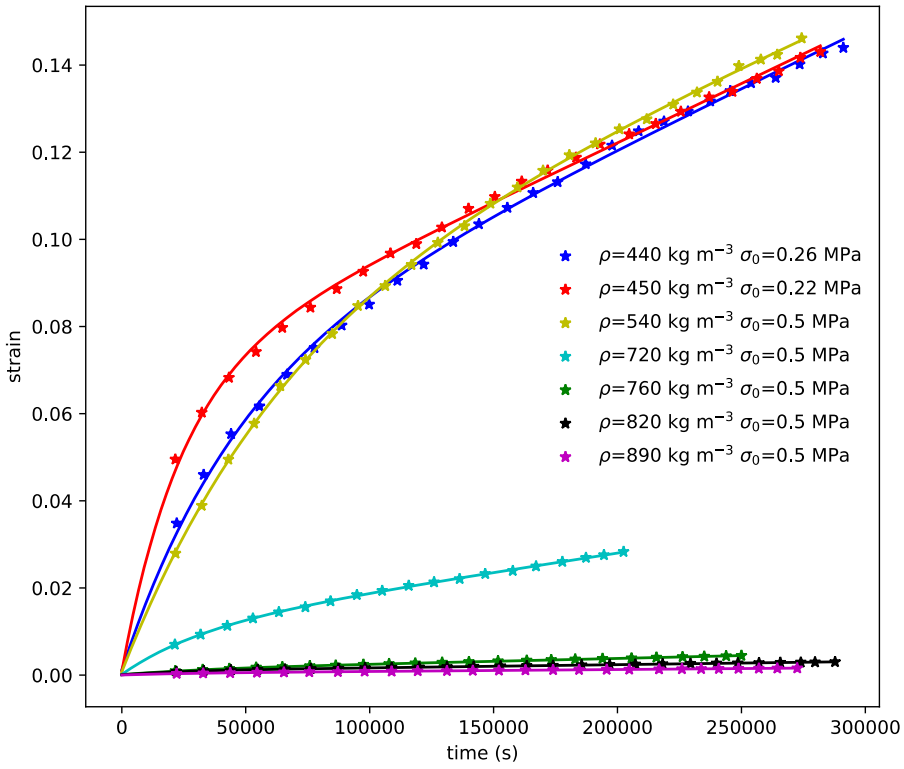

Figure 5. Creep-model predictions (*solid line*) of strain against the experimental data set from Chandel et al. (2007) (*asterisk*) for a variety of snow temperatures. The snow density was 450 kg m^{-3}, and the external load was 15 kPa for all samples.

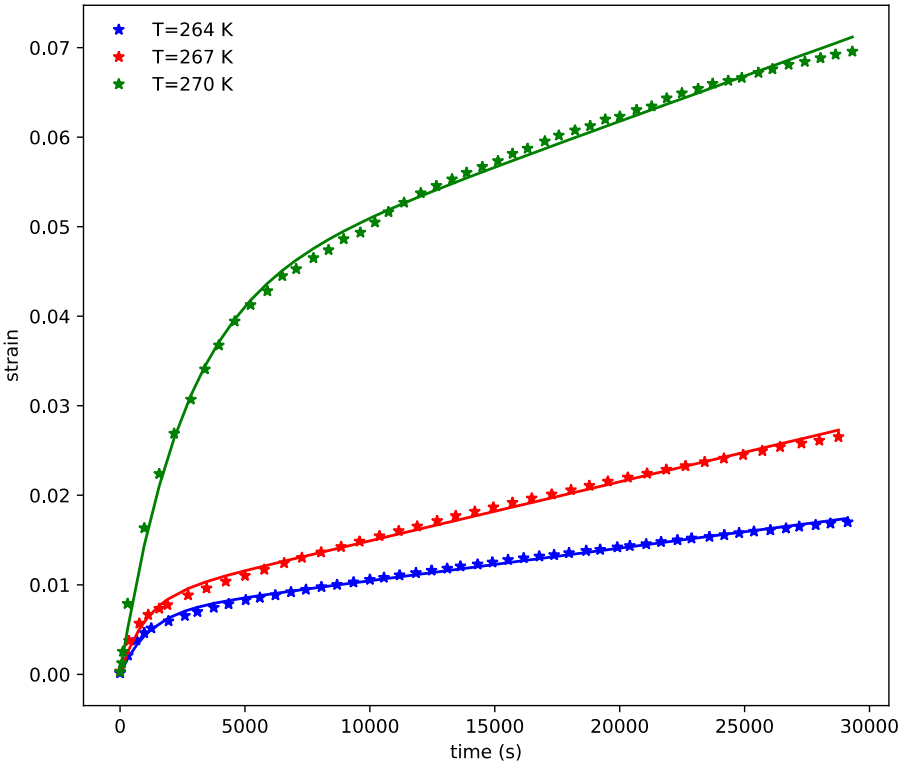

Figure 6. Secondary-creep-model predictions (*solid line*) of strain rate against the experimental data set from Mellor and Smith (1966) (*asterisk*). The external load was 49.1 kPa for all samples.

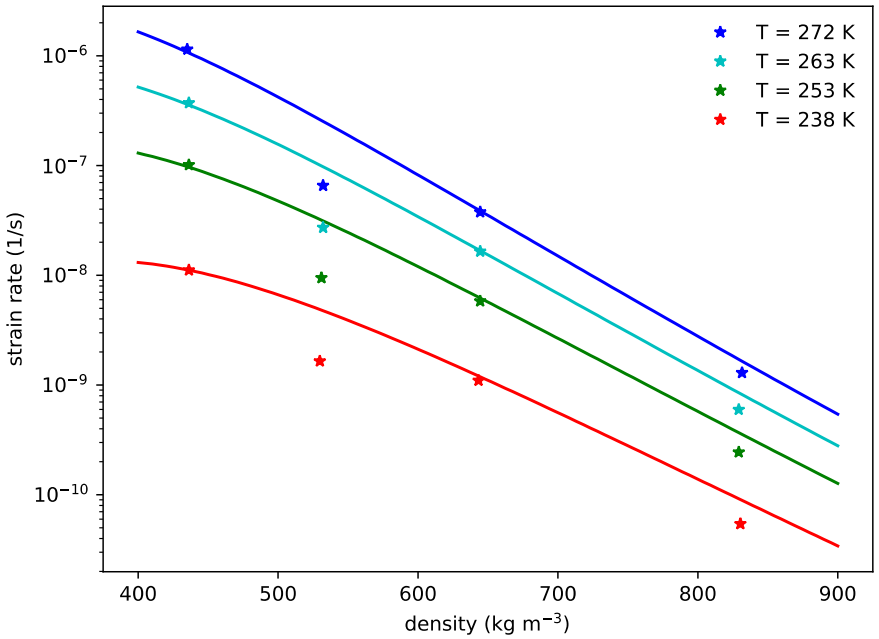

The Figures 7, 8, and 9 display the data from the fitting, indicated with asterisks, for $A_0(\rho)$, $B_0(\rho)$, and $K(\rho)$. The strain-rate data from Mellor and Smith (1966) is representative of long-term viscous strain from secondary creep only. Therefore, we calculated values for only the constant $B_0(\rho)$ in the viscous-strain model that fit the data. Using the power-law models from equations (18), (19), and (20), we once again performed a least-squares fitting to find values for A_{01}, A_{02}, B_{01}, B_{02}, K_1, and K_2 that best fit the data. As seen from the figures, there is a fair amount of scatter in the data. That is reflected in the R^2 values calculated from the least-squares fitting. For the A_0 model, the R^2 value was 0.23; the B_0 model value was 0.44; and finally, the K model value was 0.19. We would expect this large amount is scatter in the data because we are combining parameters from three different data sets. We would also expect some amount of uncertainty in the experiments and our model that is not being accounted for here in this deterministic approach. Nonetheless, our power-law models capture the overall trend in the parameters $A_0(\rho)$, $B_0(\rho)$, and $K(\rho)$.

Figure 7. Parameter values for the delayed-elastic-strain model determined from least-squares fitting to experimental data (*asterisks*). The *solid line* shows the power-law model for A_0 that best fits the data.

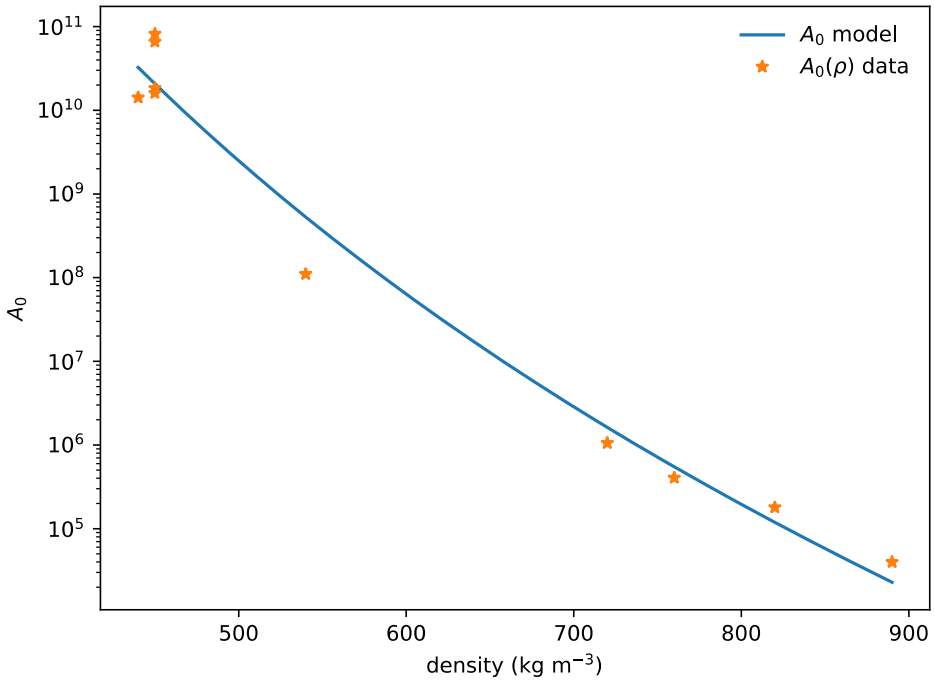

Figure 8. Parameter values for the viscous-strain model determined from least-squares fitting to experimental data (*asterisks*). The *solid line* shows the power-law model for B_0 that best fits the data.

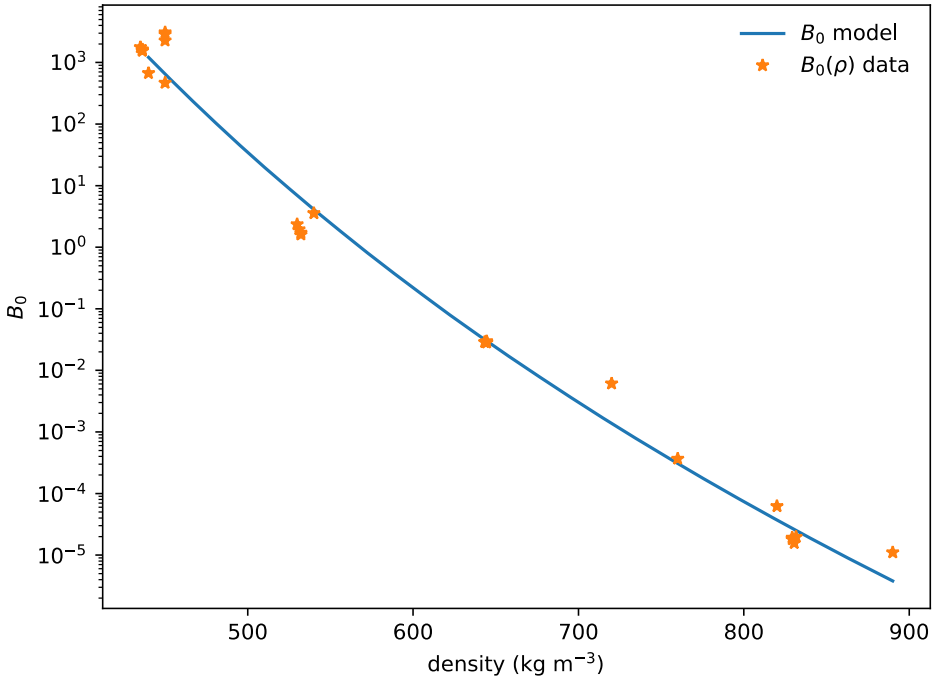

Figure 9. Parameter values for the delayed-elastic-strain model determined from least-squares fitting to experimental data (*asterisks*). The *solid line* shows the power-law model for K that best fits the data.

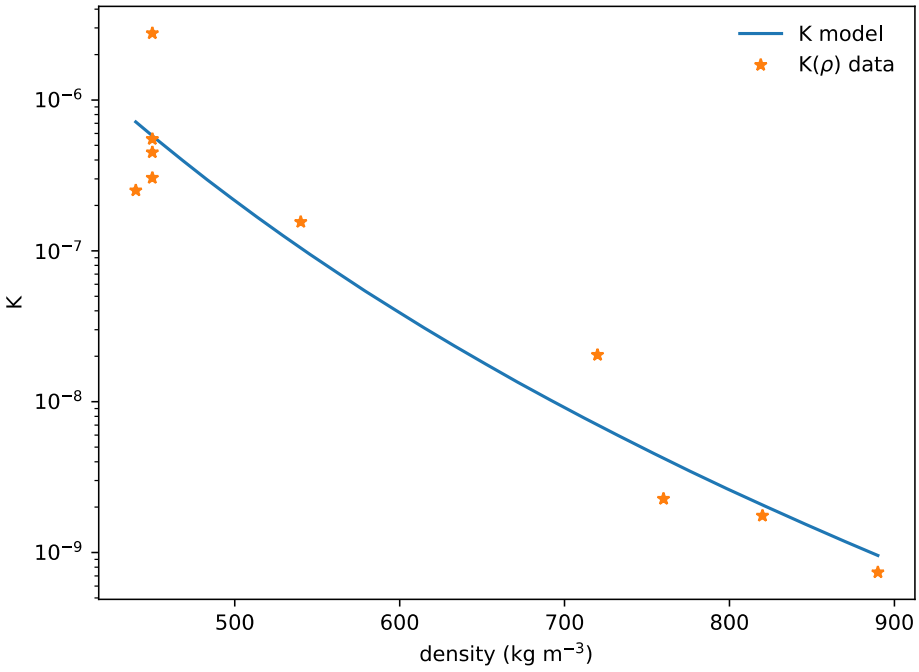

Additional snow creep data would help illuminate the effectiveness of the modeling approach and the choice of functional form for the empirical parameters. Table 1 shows the values calculated from the fitting of the empirical parameter models.

Table 1. Empirical model parameters calculated from least-squares fitting of experimental creep compression data.

A_{01}	A_{02}	B_{01}	B_{02}	K_1	K_2
4.804×10^{63}	−20.11	3.693×10^{76}	−27.80	4.808×10^{18}	−9.39

The parameterized snow creep model was implemented as an ABAQUS user material model. The next section discusses the ABAQUS model verification.

3 Finite Element Model Verification

The snow creep model laid out in the previous sections was implemented in an ABAQUS user material model. Appendix A provides the user material model in its entirety. The ABAQUS implementation is based off of the equations in the finite element implementation discussion in section 2.2.

To verify that our creep-model implementation in ABAQUS was correct, we compared our simulation results to the one-dimensional analytical creep strain seen in equation (15). The ABAQUS model was a single finite element model with symmetric boundary conditions to ensure a uniaxial response. A creep stress of 15 kPa was applied in all simulations at a snow temperature of −9°C. We varied the snow density from 450 kg m^{-3} to 850 kg m^{-3} in increments of 100. Figure 10 and Figure 11 show the results, which compare well with the analytical results as expected. Note that the results were split into two figures to easily see the comparison against the analytical model. Given small enough load steps, the ABAQUS results should converge to the analytical model.

Figure 10. Simulation results compared to analytical snow creep model for densities of 450 kg m^{-3} and 550 kg m^{-3}.

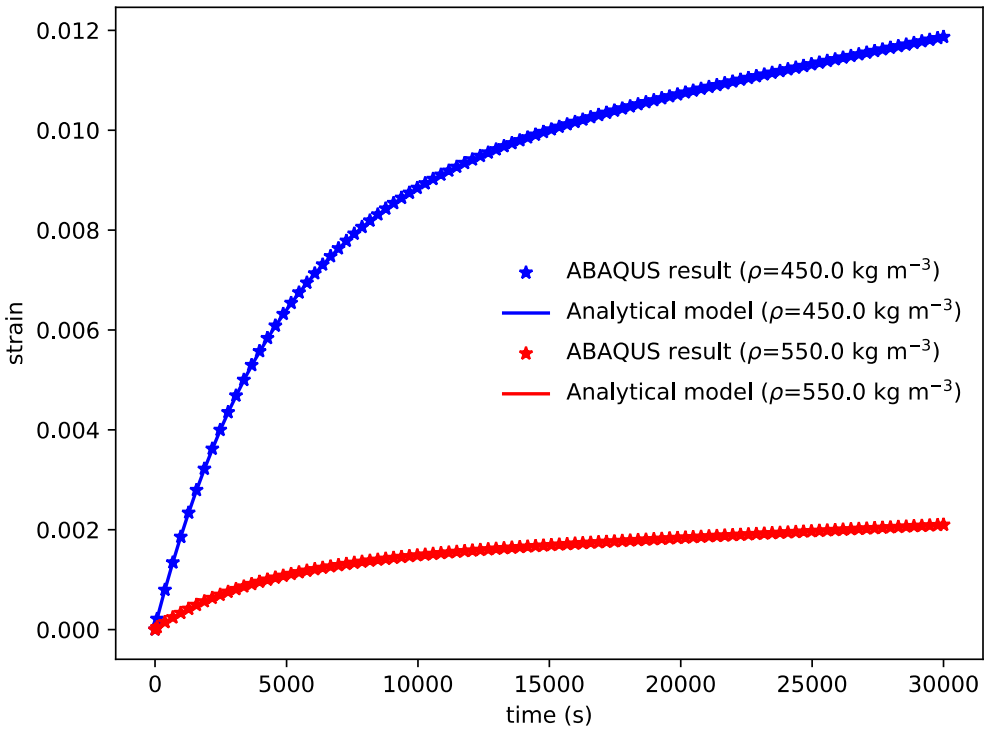

Figure 11. Simulation results compared to the analytical snow creep model for densities of 650 kg m^{-3}, 750 kg m^{-3}, and 850 kg m^{-3}.

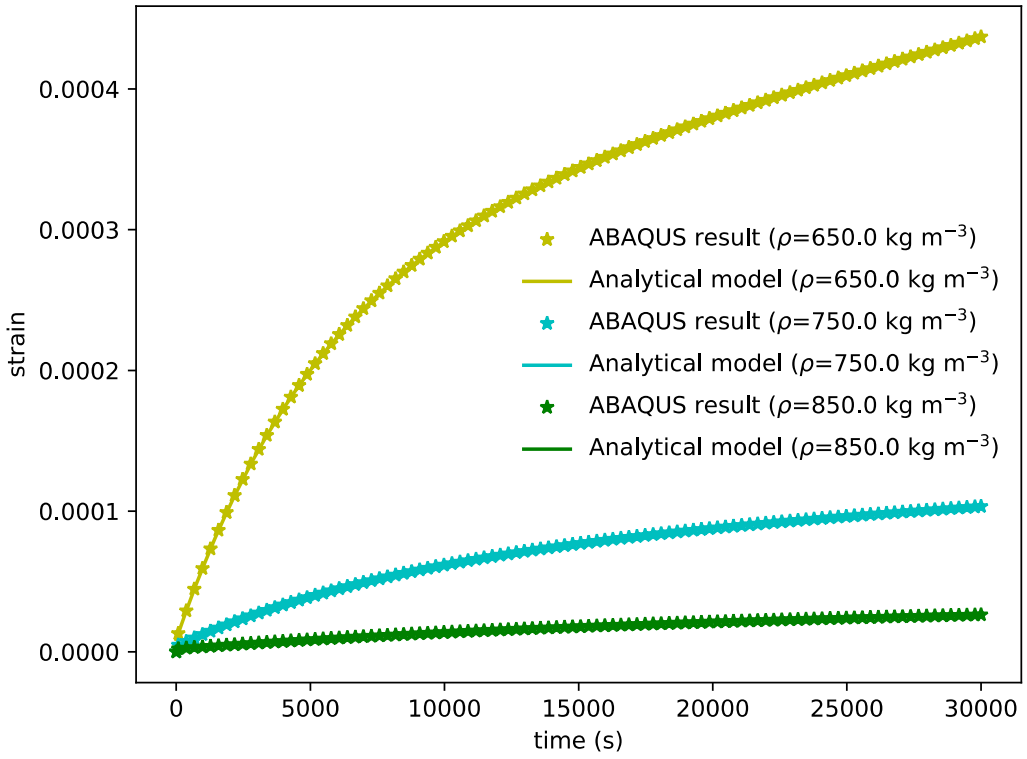

4 Results

4.1 Uniaxial snow creep

To validate our creep modeling approach, we tested our method against two experimental data sets from Theile et al. (2011). They performed two uniaxial compressive creep tests on snow at a temperature of –11°C with cylindrical samples. The first test, referred to as Sample 1 in Figure 12, had an initial density of 205 kg m^{-3} and was compressed with a 2 kPa load while the second test, referred to as Sample 2 in Figure 12, had an initial density of 270 kg m^{-3} and was compressed with a 10 kPa load. The authors measured and reported the initial density and final density after compression for each sample.

Figure 12. Snow creep model (*solid line*) compared with two uniaxial compressive creep tests (*asterisks*) from Theile et al. (2011) shown on a log-log scale.

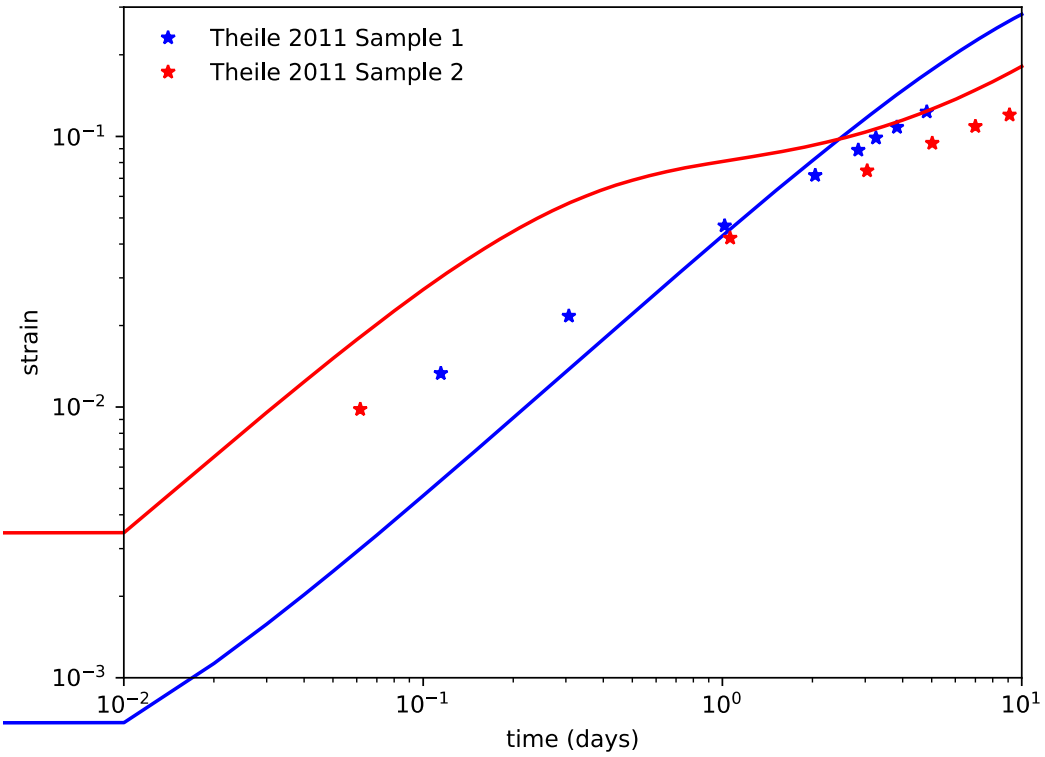

Our model needs to use a temporally constant density as our method currently does not allow the density to change in time. For both Samples 1 and 2, we chose to use the final densities in our analysis, which were 240 kg m^{-3} and 345 kg m^{-3}, respectively. For validation simulations, we used the model parameters outlined in the previous sections and the density, temperature, and compressive loading values for each snow sample.

In general, the snow creep model is set up such that the only inputs are the density and temperature of the snow and the boundary conditions (e.g., external compressive load). Figure 12 compares the modeling results to the two snow sample data sets. As the figure shows, the model matches the overall trend in the strain data well, even predicting the total strain towards the end of the experiment fairly well. Considering contributions of uncertainty to the model and experiment, it is unrealistic to expect the model to match the data exactly when using a deterministic approach. For example, see the scatter in replicate samples 3.1, 3.2, and 3.3 presented in Theile et al. (2011). Also, since we used the final time density, it is unsurprising that the error between our model and the data is the smallest towards the end of the experiment.

4.2 Secondary snow creep

To continue our validation efforts, we compared the strain-rate response of our model against the experimental results from Mellor and Smith (1966).

They tested cylindrical snow samples in uniaxial compression for a number of densities (436 kg m^{-3} through 832 kg m^{-3}), temperatures (–1°C through –35°C), and applied compressive loads (49.1 kPa and 98.1 kPa). Figure 13 shows the experimental results, displayed as asterisks, of the strain rate plotted against temperature. Test durations were on the order of 115 days; and we expected, based on the level loading and time, that most of the strain in the snow would be due to secondary creep effects. Therefore, we chose to use a subset of our model, the viscous-strain model, seen in equation (7) to compare with the experimental results. Note that the uniaxial version of equation (7) is

$$\dot{\varepsilon}^v = B_{01}\rho^{B_{02}} \exp\left(-\frac{Q_1\rho^{Q_2}}{RT}\right)\sigma^n, \tag{21}$$

where all constants have been defined previously. Using our snow creep model, we simulated the snow creep experiments of Mellor and Smith (1966) (Figure 13). As the figure shows, we matched the overall trend in the data quite well with the exception of the tests at a density of 531 kg m^{-3}. It is hard to say why the model does not capture the response of the snow at that density for these experiments. There could be an issue with those experiments or there is some physical mechanism that operates at that snow density that the model does not capture. In any case, the model captures the secondary snow creep results of Mellor and Smith (1966) well.

Figure 13. Secondary-creep-model predictions (*solid line*) of strain rate against the experimental data set from Mellor and Smith (1966) (*asterisks*).

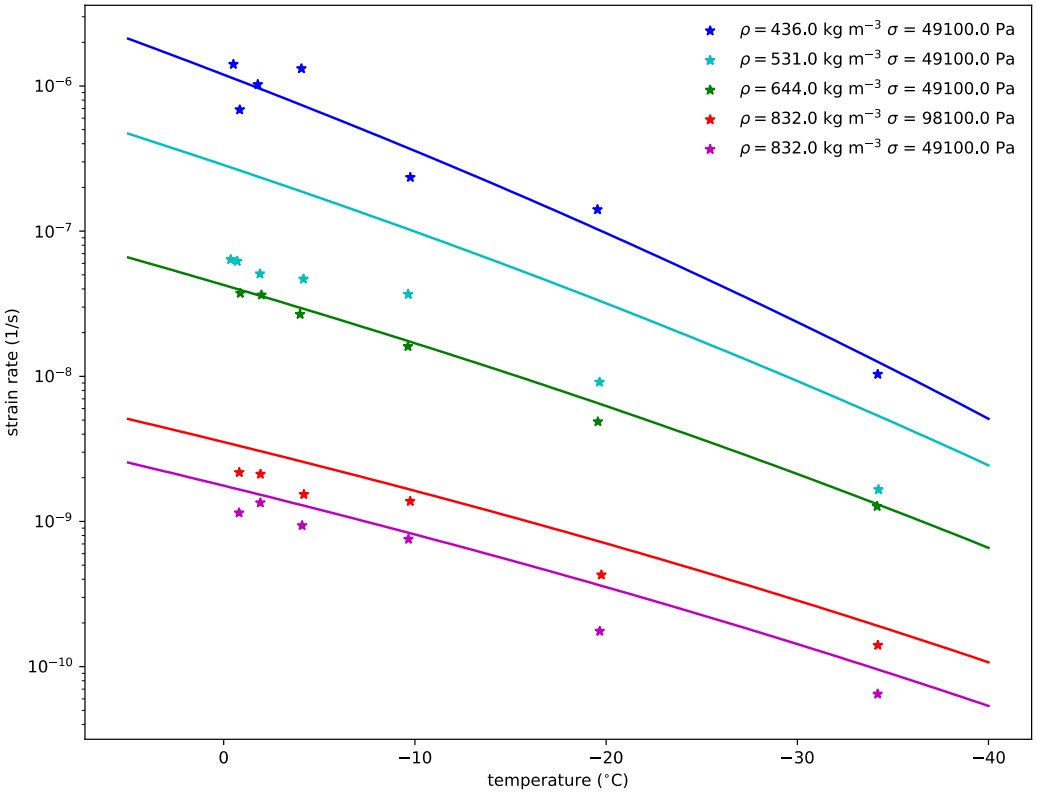

5 Discussion and Conclusions

In this report, we developed a general model for the creep behavior of snow. This new approach spans both the primary and secondary regimes of creep known to be induced when loading snow foundations. We based our model initially on the uniaxial rheological Burgers model but extended that implementation to three dimensions and changed the parameterization to have density- and temperature-dependent constants as both have strong influences over the creep of snow. Minimizing the misfit between our model predictions and experimental data of snow creep, we estimated the parameters of our model that best describe the creep strain data. Additionally, we presented a finite element implementation of our model and the method to include it in an ABAQUS user material model. We verified the user material model against an analytical version of our creep model and validated our creep model against additional experimental creep data sets. The results showed that our model can match the data well over different time scales, temperatures, densities, and external loads.

Depending on the duration of loading of a snow foundation, the majority of straining could be due to primary creep or to a combination of primary and secondary mechanisms. Besides the magnitude of loading, the temperature and density of the snow influence the time at which the strain transitions from primary to secondary creep. For example, under a uniaxial load of 15 kPa, a snow temperature of –30°C, and a density 650 kg m^{-3}, our model predicts a transition to secondary creep at approximately 1.5 days. Putting this in context, the snow foundation for the Greenland Telescope is expected to deform according to secondary-creep theory based on the loading time (Haehnel 2017). Although, during a telescope pointing operation, which lasts about 8 hours, the load on the snow foundation can increase; and primary-creep straining could be induced. Knowledge of the transition from primary to secondary creep can help better understand snow foundation performance.

While our modeling approach shows promise, future work will need to consider sources of uncertainty (e.g., from both the model and the experiments) to more accurately estimate snow foundation creep. For example, we parameterize our model using experimental data sets, which in general have some scatter that we are not accounting for. Furthermore, additional snow creep data is needed to help identify sources and amounts of

uncertainty in our model formulation and model parameters. Finally, additional validation against field data will increase the robustness of the modeling approach.

The model developed in this work can estimate snow foundation creep with knowledge of only the snow density, temperature, and external load. The uniaxial creep equation shown in equation (15) can provide a good estimate of snow foundation deformation in situations where uniaxial deformation is a safe assumption. In more complicated situations, where more complex structures are placed on snow, the user material model can be used in combination with the finite element software ABAQUS to estimate both snow deformation over time and the foundation's performance. As interests in the Arctic and Antarctic increase (militarily, commercially, or otherwise), the need for infrastructure built on snow foundations will increase as well. The model we developed to estimate snow creep deformation is needed to build safe and long-lasting structures.

References

Bartelt, P., and M. Christen. 2007. "A Computational Procedure for Instationary Temperature-Dependent Snow Creep." In *Advances in Cold-Region Thermal Engineering and Sciences*, 367–86. Berlin: Springer-Verlag. https://doi.org/10.1007/bfb0104195.

Chandel, C., P. K. Srivastava, and P. Mahajan. 2014. "Micromechanical Analysis of Deformation of Snow Using X-Ray Tomography." *Cold Regions Science and Technology* 101:14–23. https://doi.org/10.1016/j.coldregions.2014.01.005.

Chandel, C., P. K. Srivastava, and A. Upadhyay. 2007. "Estimation of Rheological Properties of Snow Subjected to Creep." *Defence Science Journal* 57 (4): 539–47. https://doi.org/10.14429/dsj.57.1786.

Duddu, R., and H. Waisman. 2012. "A Temperature Dependent Creep Damage Model for Polycrystalline Ice." *Mechanics of Materials* 46:23–41. https://doi.org/10.1016/j.mechmat.2011.11.007.

———. 2013. "A Nonlocal Continuum Damage Mechanics Approach to Simulation of Creep Fracture in Ice Sheets." *Computational Mechanics* 51 (6): 961–74. https://doi.org/10.1007/s00466-012-0778-7.

Ghaboussi, J., and R. Barbosa. 1990. "Three-Dimensional Discrete Element Method for Granular Materials." *International Journal for Numerical and Analytical Methods in Geomechanics* 14 (7): 451–72. https://doi.org/10.1002/nag.1610140702.

Haehnel, R.B. 2017. *A Creep Model for High-Density Snow*. ERDC/CRREL TR-17-7. Hanover, NH: U.S. Army Engineer Research and Development Center. https://apps.dtic.mil/dtic/tr/fulltext/u2/1036422.pdf.

Hagenmuller, P., G. Chambon, and M. Naaim. 2015. "Microstructure-Based Modeling of Snow Mechanics: A Discrete Element Approach." *Cryosphere* 9 (5): 1969–82. https://doi.org/10.5194/tc-9-1969-2015.

Johnson, J. B, and M. A Hopkins. 2005. "Identifying Microstructural Deformation Mechanisms in Snow Using Discrete-Element Modeling." *Journal of Glaciology* 51 (174): 432–42. https://doi.org/10.3189/172756505781829188.

Karr, D. G., and K. Choi. 1989. "A Three-Dimensional Constitutive Damage Model for Polycrystalline Ice." *Mechanics of Materials* 8 (1): 55–66. https://doi.org/10.1016/0167-6636(89)90005-7.

Köhle, B., and M. Schneebeli. 2014. "Three-Dimensional Microstructure and Numerical Calculation of Elastic Properties of Alpine Snow with a Focus on Weak Layers." *Journal of Glaciology* 60 (222): 705–13. https://doi.org/10.3189/2014JoG13J220.

Kozin, V. M., V. L. Zemlyak, V. Y. Vereshchagin. 2013. "Influence of Snow Cover on the Parameters Flexural-Gravity Waves in Ice Cover." *Journal of Applied Mechanics and Technical Physics* 54 (3): 458–64. https://doi.org/10.1134/S0021894413030152.

Londono, J. G., L. Berger-Vergiat, and H. Waisman. 2016. "A Prony-Series Type Viscoelastic Solid Coupled with a Continuum Damage Law for Polar Ice Modeling." *Mechanics of Materials* 98:81–97. https://doi.org/10.1016/j.mechmat.2016.04.002.

Mellor, M. 1964. *Properties of Snow*. Hanover, NH: U.S. Army Cold Regions Research and Engineering Laboratory. http://hdl.handle.net/11681/2633.

———. 1975. "A Review of Basic Snow Mechanics." In *The International Symposium on Snow Mechanics,* Grindewald, Switzerland, 1–5 April 1974. IAHS-AISH Publication 114, 251–291. International Association of Hydrological Sciences, Snow and Ice Commission. http://hydrologie.org/redbooks/a114/iahs_114_0251.pdf.

Mellor, M., and H. J. Smith. 1966. *Creep of Snow and Ice*. Research Report 220. Hanover, NH: U.S. Army Cold Regions Research and Engineering Laboratory. http://hdl.handle.net/11681/5879.

Meussen, B., O. Mahrenholtz, and H. Oerter. 1999. "Creep of Polar Firn." *Cold Regions Science and Technology* 29 (3): 177–200. https://doi.org/10.1016/S0165-232X(99)00018-X.

Navarre, J. P., J. Meyssonnier, and A. Vagnon. 2007. "3D Numerical Model of Snow Deformation without Failure and Its Application to Cold Room Mechanical Tests." *Cold Regions Science and Technology* 50 (1–3): 3–12. https://doi.org/10.1016/j.coldregions.2007.04.002.

Ohno, N., S. Murakami, and T. Ueno. 1985. "A Constitutive Model of Creep Describing Creep Recovery and Material Softening Caused by Stress Reversals." *Journal of Engineering Materials and Technology, Transactions of the ASME* 107 (1): 1–6. https://doi.org/10.1115/1.3225766.

Salm, B. 1982. "Mechanical Properties of Snow." *Reviews of Geophysics* 20 (1): 1–19. https://doi.org/10.1029/RG020i001p00001.

Shapiro, L. H., J. B. Johnson, M. Sturm, and G. L. Blaisdell. 1997. *Snow Mechanics: Review of the State of Knowledge and Applications*. CRREL Report 97-3. Hanover, NH: U.S. Army Cold Regions Research and Engineering Laboratory. http://hdl.handle.net/11681/9238.

Srivastava, P. K., C. Chandel, P. Mahajan, and P. Pankaj. 2016. "Prediction of Anisotropic Elastic Properties of Snow from Its Microstructure." *Cold Regions Science and Technology* 125: 85–100. https://doi.org/10.1016/j.coldregions.2016.02.002.

Teufelsbauer, H. 2011. "A Two-Dimensional Snow Creep Model for Alpine Terrain." *Natural Hazards* 56 (2): 481–97. https://doi.org/10.1007/s11069-010-9515-8.

Theile, T., H. Löwe, T. C. Theile, and M. Schneebeli. 2011. "Simulating Creep of Snow Based on Microstructure and the Anisotropic Deformation of Ice." *Acta Materialia* 59 (18): 7104–13. https://doi.org/10.1016/j.actamat.2011.07.065.

Vedachalam, V. 2011. *Discrete Element Modelling of Granular Snow Particles Using Liggghts*. M. Sc., University of Edinburgh. https://static.epcc.ed.ac.uk/dissertations/hpc-msc/2010-2011/VinodhVedachalam.pdf.

Xu, Y., Z. Hu, J. W. Ringsberg, and G. Chen. 2019. "Nonlinear Viscoelastic-Plastic Material Modelling for the Behaviour of Ice in Ice-Structure Interactions." *Ocean Engineering* 173 (April 2018): 284–97. https://doi.org/10.1016/j.oceaneng.2018.12.050.

Yoshida, Z. 1955. "Physical Studies on Deposited Snow. I.; Thermal Properties." *Contributions from the Institute of Low Temperature Science* 7:19–74. http://hdl.handle.net/2115/20216.

Appendix A: ABAQUS User Material Model

Below is the FORTRAN ABAQUS user material model that we created to model snow creep.

```
C ----------------------------------------------------------------------
C     ABAQUS UMAT for Snow Mechanics (Creep)
C
C     Author: Devin T. O'Connor
C     Institution: Cold Regions Research and Engineering Laboratory
C     Last updated: 23 September 2019
C ----------------------------------------------------------------------

      SUBROUTINE UMAT(STRESS, STATEV, DDSDDE, SSE, SPD, SCD, RPL,
     1 DDSDDT, DRPLDE, DRPLDT, STRAN, DSTRAN, TIME, DTIME, TEMP, DTEMP,
     2 PREDEF, DPRED, CMNAME, NDI, NSHR, NTENS, NSTATV, PROPS, NPROPS,
     3 COORDS, DROT, PNEWDT, CELENT, DFGRD0, DFGRD1, NOEL, NPT, LAYER,
     4 KSPT, KSTEP, KINC)

      INCLUDE 'ABA_PARAM.INC'

      CHARACTER*8 CMNAME

      DIMENSION STRESS(NTENS), STATEV(NSTATV), DDSDDE(NTENS, NTENS),
     1 DDSDDT(NTENS), DRPLDE(NTENS), STRAN(NTENS), DSTRAN(NTENS),
     2 PREDEF(1), DPRED(1), PROPS(NPROPS), COORDS(3), DROT(3, 3),
     3 DFGRD0(3, 3), DFGRD1(3, 3)

C ----------------------------------------------------------------------
C     Local variables and arrays
C ----------------------------------------------------------------------
C     E - Elastic modulus
C     Q - Activation energy
C     K - Delayed elastic strain constant
C     A - Delayed elastic strain constant
C     B - Viscous strain constant
C     STRESS_TR - Trace of the stress tensor
C     STRESS_DEV - Deviatoric stress
C     STRESS_DEV_SQ_LEN - Devatoric stress inner product
C     STRESS_VM -  Von Mises stress
C     STRAIN_A_INC - Delayed elastic strain increment
C     STRAIN_A_OLD - Delayed elastic strain from previous solution
C     STRAIN_V_INC - Viscous strain increment
C ----------------------------------------------------------------------

      INTEGER K1, K2

      REAL*8 E, Q, K, A, B, STRESS_TR, STRESS_DEV, STRESS_DEV_SQ_LEN,
     1 STRESS_VM, STRAIN_A_INC, STRAIN_A_OLD, STRAIN_V_INC

      DIMENSION STRESS_DEV(NTENS), STRAIN_A_INC(NTENS),
     1 STRAIN_A_OLD(NTENS), STRAIN_V_INC(NTENS)

C ----------------------------------------------------------------------
```

```
C     User input constitutive model properties
C ------------------------------------------------------------------
C     PROPS(1) - RHO (Snow density)
C     PROPS(2) - T (Snow temperature)
C ------------------------------------------------------------------

C ------------------------------------------------------------------
C     User defined constitutive model properties
C ------------------------------------------------------------------
C     E_1 - elastic modulus constant 1
C     E_2 - elastic modulus constant 2
C     Q_1 - activation energy constant 1
C     Q_2 - activation energy constant 2
C     K_1 - Delayed elastic strain constant K 1
C     K_2 - Delayed elastic strain constant K 2
C     A0_1 - Delayed elastic strain constant A0 1
C     A0_2 - Delayed elastic strain constant A0 2
C     B0_1 - Delayed elastic strain constant B0 1
C     B0_2 - Delayed elastic strain constant B0 2
C     NU - Poisson's ratio
C     R - Gas constant
C     N - Viscous strain exponent
C ------------------------------------------------------------------

      REAL*8 RHO, T, E_1, E_2, Q_1, Q_2, K_1, K_2, A0_2, B0_2, NU, R, N
      REAL*16 A0_1, B0_1

      RHO = PROPS(1)
      T = PROPS(2)

      E_1 = 1.99884211D-6
      E_2 = 5.30708127
      Q_1 = 1.14522618D3
      Q_2 = -0.690446294
      K_1 = 4.80783132D18
      K_2 = -9.39216585
      A0_1 = 4.80353109D63
      A0_2 = -20.1133237
      B0_1 = 3.6928674D76
      B0_2 = -27.797909
      NU = 0.3
      R = 1.985877534D-3
      N = 1.0

C ------------------------------------------------------------------
C     State variables
C ------------------------------------------------------------------
C     STATEV(1) - Delayed elastic strain component 11
C     STATEV(2) - Delayed elastic strain component 22
C     STATEV(3) - Delayed elastic strain component 33
C     STATEV(4) - Delayed elastic strain component 23
C     STATEV(5) - Delayed elastic strain component 13
C     STATEV(6) - Delayed elastic strain component 12
C
C     For plane strain or axisymmetric elements
C     -----------------------------------------
C     STATEV(1) - Delayed elastic strain component 11
```

```
C     STATEV(2) - Delayed elastic strain component 22
C     STATEV(3) - Delayed elastic strain component 33
C     STATEV(4) - Delayed elastic strain component 12
C ------------------------------------------------------------------

C ------------------------------------------------------------------
C     User Defined Field Snow Density
C ------------------------------------------------------------------

C     Override constant density with user defined field
C     To override uncomment RHO definition below

C      RHO = PREDEF(1)

C ------------------------------------------------------------------
C     Define old delayed elastic strain from pervious step
C ------------------------------------------------------------------

      DO K1 = 1, NTENS
        STRAIN_A_OLD(K1) = STATEV(K1)
      END DO

C ------------------------------------------------------------------
C    Elastic modulus
C ------------------------------------------------------------------

      E = E_1*RHO**E_2

C ------------------------------------------------------------------
C    Activation Energy
C ------------------------------------------------------------------

      Q = Q_1*RHO**Q_2

C ------------------------------------------------------------------
C    Experimentally determined constants
C ------------------------------------------------------------------

      K = K_1*RHO**K_2

      A = A0_1*RHO**A0_2*EXP(-Q/(R*T))

      B = B0_1*RHO**B0_2*EXP(-Q/(R*T))

C ------------------------------------------------------------------
C    Stress based constants and arrays
C ------------------------------------------------------------------

C     Trace of the stress tensor
      STRESS_TR = 0.0
      DO K1 = 1, NDI
        STRESS_TR = STRESS_TR + STRESS(K1)
      END DO

C     Deviatoric stress
      DO K1 = 1, NDI
        STRESS_DEV(K1) = STRESS(K1) - STRESS_TR/3.0
```

```
      END DO
      DO K1 = NDI+1, NTENS
        STRESS_DEV(K1) = STRESS(K1)
      END DO

C     Deviatoric stress inner product (sig_mn * sig_mn)
      STRESS_DEV_SQ_LEN = 0.0
      DO K1 = 1, NDI
        STRESS_DEV_SQ_LEN = STRESS_DEV_SQ_LEN + STRESS_DEV(K1)**2
      END DO
      DO K1 = NDI+1, NTENS
        STRESS_DEV_SQ_LEN = STRESS_DEV_SQ_LEN + 2.0*STRESS_DEV(K1)**2
      END DO

C     Von Mises stress
      STRESS_VM = (3.0/2.0*STRESS_DEV_SQ_LEN)**0.5

C ---------------------------------------------------------------------
C     Linear isotropic stiffness tensor
C ---------------------------------------------------------------------

      DDSDDE(:, :) = 0.0
      DO K1 = 1, NDI
        DO K2 = 1, NDI
          DDSDDE(K1, K2) = NU*E/((1.0+NU)*(1.0-2.0*NU))
        END DO
        DDSDDE(K1, K1) = (1.0-NU)*E/((1.0+NU)*(1.0-2.0*NU))
      END DO
      DO K1 = NDI+1, NTENS
        DDSDDE(K1 ,K1) = 0.5*E/(1.0+NU)
      END DO

C ---------------------------------------------------------------------
C     Delayed elastic strain increment
C ---------------------------------------------------------------------

      DO K1 = 1, NTENS
        STRAIN_A_INC(K1) = A*DTIME*(3.0/2.0*K*STRESS_DEV(K1) -
     1                              STRAIN_A_OLD(K1))
      END DO

C ---------------------------------------------------------------------
C     Viscous strain increment
C ---------------------------------------------------------------------

      DO K1 = 1, NTENS
        STRAIN_V_INC(K1) = 3.0/2.0*B*DTIME*STRESS_DEV(K1)*
     1                     STRESS_VM**(N-1)
      END DO

C ---------------------------------------------------------------------
C     Update stress
C ---------------------------------------------------------------------

      DO K1 = 1, NTENS
        DO K2 = 1, NTENS
          STRESS(K1) = STRESS(K1) + DDSDDE(K1, K2)*(DSTRAN(K2) -
```

```
     1                                                  STRAIN_A_INC(K2) -
     2                                                  STRAIN_V_INC(K2))

       END DO
      END DO

C -------------------------------------------------------------------------
C     Update state variables (delayed elastic strain)
C -------------------------------------------------------------------------

      DO K1 = 1, NTENS
        STATEV(K1) = STRAIN_A_OLD(K1) + STRAIN_A_INC(K1)
      END DO

      RETURN
      END
```

REPORT DOCUMENTATION PAGE

Form Approved
OMB No. 0704-0188

1. REPORT DATE *(DD-MM-YYYY)*	2. REPORT TYPE	3. DATES COVERED *(From - To)*
May 2020	Technical Report/Final	

4. TITLE AND SUBTITLE

A Generalized Approach for Modeling Creep of Snow Foundations

5a. CONTRACT NUMBER

5b. GRANT NUMBER

5c. PROGRAM ELEMENT NUMBER

6. AUTHOR(S)

Devin T. O'Connor and Robert B. Haehnel

5d. PROJECT NUMBER

5e. TASK NUMBER

5f. WORK UNIT NUMBER

7. PERFORMING ORGANIZATION NAME(S) AND ADDRESS(ES)

U.S. Army Engineer Research and Development Center (ERDC)
Cold Regions Research and Engineering Laboratory (CRREL)
72 Lyme Road
Hanover, NH 03755-1290

8. PERFORMING ORGANIZATION REPORT NUMBER

ERDC/CRREL TR-20-4

9. SPONSORING / MONITORING AGENCY NAME(S) AND ADDRESS(ES)

National Science Foundation
Office of Polar Programs
Antarctic Infrastructure and Logistics
2415 Eisenhower Avenue
Alexandria, VA 22314

10. SPONSOR/MONITOR'S ACRONYM(S)

11. SPONSOR/MONITOR'S REPORT NUMBER(S)

12. DISTRIBUTION / AVAILABILITY STATEMENT

Approved for public release; distribution is unlimited.

13. SUPPLEMENTARY NOTES

Engineering for Polar Operations, Logistics, and Research (EPOLAR) EP-ANT-18-85, "A Generalized Approach for Modeling Creep of Snow Foundations"

14. ABSTRACT

When an external load is applied, snow will continue to deform in time, or creep, until the load is removed. When using snow as a foundation material, one must consider the time-dependent nature of snow mechanics to understand its long-term structural performance. In this work, we develop a general approach for predicting the creep behavior of snow. This new approach spans the primary (nonlinear) to secondary (linear) creep regimes. Our method is based on a uniaxial rheological Burgers model and is extended to three dimensions. We parameterize the model with density- and temperature-dependent constants that we calculate from experimental snow creep data. A finite element implementation of the multiaxial snow creep model is derived, and its inclusion in an ABAQUS user material model is discussed. We verified the user material model against our analytical snow creep model and validated our model against additional experimental data sets. The results show that the model captures the creep behavior of snow over various time scales, temperatures, densities, and external loads. By furthering our ability to more accurately predict snow foundation movement, we can help prevent unexpected failures and extend the useful lifespan of structures that are constructed on snow.

15. SUBJECT TERMS

Computational Model, Cryosphere, EPOLAR, Finite element method, Foundations--Cold weather conditions, Installations, NSF, Polar Science and Engineering, Snow, Snow Creep, Snow Foundation, Snow Mechanics

16. SECURITY CLASSIFICATION OF:			17. LIMITATION OF ABSTRACT	18. NUMBER OF PAGES	19a. NAME OF RESPONSIBLE PERSON
a. REPORT	b. ABSTRACT	c. THIS PAGE			19b. TELEPHONE NUMBER *(include area code)*
Unclassified	Unclassified	Unclassified	SAR	39	